Eur. Phys. J. B **7**, 105–109 (1999)

THE EUROPEAN PHYSICAL JOURNAL B

EDP Sciences

Universality in three dimensional random-field ground states

A.K. Hartmann[1,a] and U. Nowak[2,b]

[1] Institut für theoretische Physik, Philosophenweg 19, 69120 Heidelberg, Germany
[2] Theoretische Tieftemperaturphysik, Gerhard-Mercator-Universität-Duisburg, 47048 Duisburg, Germany

Received: 9 July 1998 / Received in final form: 15 July 1998 / Accepted: 20 July 1998

Abstract. We investigate the critical behavior of three-dimensional random-field Ising systems with both Gauss and bimodal distribution of random fields and additional the three-dimensional diluted Ising antiferromagnet in an external field. These models are expected to be in the same universality class. We use exact ground-state calculations with an integer optimization algorithm and by a finite-size scaling analysis we calculate the critical exponents ν, β, and $\bar{\gamma}$. While the random-field model with Gauss distribution of random fields and the diluted antiferromagnet appear to be in same universality class, the critical exponents of the random-field model with bimodal distribution of random fields seem to be significantly different.

PACS. 05.70.Jk Critical point phenomena – 64.60.Fr Equilibrium properties near critical points, critical exponents – 75.10.Hk Classical spin models – 75.50.Lk Spin glasses and other random magnets

Above two dimensions, the ferromagnetic random-field Ising model (RFIM) is long-range ordered for low temperatures and small random fields as was proven by Imbrie [1] and also by Bricmont and Kupiainen [2]. For larger fields the system develops a frozen domain state [3] which has been shown to have a complex, fractal structure [4]. It is now widely believed that there is a second order phase transition from the ordered to the disordered phase in appropriate dimensions although in three dimensions a complete set of values of the critical exponents fulfilling the predicted set of scaling relations [5–7] could still not be established. *E.g.* the value of α is still controversially discussed [8].

For the replica-symmetric mean-field solution [9] it was found that the critical behavior of the RFIM depends on the kind of distribution of random fields. Later, also for random-field systems on the Bethe-lattice [10] it was demonstrated that the critical behavior depends on the distribution of random fields. Two recent letters [11,12] were addressed to the question whether this is also true in lower dimensions. Swift *et al.* [11] found clearly different critical behavior for random-field systems with a Gauss-distribution (G-RFIM) on the one hand and a bimodal distribution (B-RFIM) on the other hand in four dimensions. They could not find a clear distinction in three dimensions. Here, it were Anglès d'Auriac and Sourlas [12] who found differences for the critical behavior of the two systems mentioned above. Especially the values of the correlation length exponent ν they found to be significantly different.

[a] e-mail: `hartmann@philosoph.tphys.uni-heidelberg.de`
[b] e-mail: `uli@thp.uni-duisburg.de`

The most prominent experimental realization of a RFIM is often asserted to be the diluted Ising antiferromagnet in a field (DAFF) (for an overview see [13,14]). This system is thought to be in the same universality class as the RFIM [15,16] but if the concept of universality is violated for random-field models the question arises what values the critical exponents of a DAFF have. Therefore, in this work we investigate these three types of random-field systems mentioned above in three dimensions and we determine at a time three of the critical exponents, ν, β and $\bar{\gamma}$ numerically in order to test if there is possibly a violation of universality. Especially the DAFF is examined the first time in this way at all.

The Hamiltonian of the RFIM in units of the exchange coupling constant is

$$H = -\sum_{\langle i,j\rangle} \sigma_i\sigma_j - \sum_i B_i\sigma_i. \tag{1}$$

The first sum is over the ferromagnetic nearest-neighbor interactions and the spin variables σ_i are $\pm$ 1. The random fields B_i are taken either from a Gauss-probability distribution $P(B_i) \sim \exp(-(B_i/\Delta)^2/2)$ or from a bimodal distribution $B_i = \pm\Delta$. In either distributions Δ scales the strength of the random field.

The corresponding Hamiltonian of the DAFF is

$$H = \sum_{\langle i,j\rangle} \epsilon_i\sigma_i\epsilon_j\sigma_j - \Delta\sum_i \epsilon_i\sigma_i \tag{2}$$

where we have now an antiferromagnetic nearest neighbor coupling and the $\epsilon_i = 0, 1$ represent the dilution. The homogenous magnetic field Δ breaks the antiferromagnetic

long-range order and in connection with the dilution it acts as random field [15,16]. Note, that for the DAFF the value of the critical Δ depends on the dilution of the system (see also [17] for a sketch of the phase diagram of the DAFF).

As was shown by renormalization group arguments [5, 18], the three-dimensional RFIM has a zero temperature fixed point at a finite value Δ_c of the random-field width and the temperature T is an irrelevant variable. Hence, we can use exact ground-state calculations to investigate the critical behavior of our systems at zero temperature.

For our numerical investigation we used a simple cubic lattice with periodical boundary conditions and linear lattice sizes varying from $L = 10$ to $L = 80$ for the RFIMs and from $L = 20$ to $L = 120$ for the DAFF. We used well-known algorithms from graph theory [19–21] to calculate the ground state of a system at given field Δ. The calculation works by transforming the system into a network [22], and calculating the maximum flow in polynomial time [23,24][1].

This method works only for systems without bond-frustration, so that spin glasses cannot be treated in this way. For most of those systems only algorithms with exponential time complexity are known, for example the Branch-and-Cut method [25,26]. For readers interested in the field we give some additional informations: Only for the special case of the two-dimensional spin glass with periodic boundary conditions in no more than one direction and without external field also a polynomial time algorithm is known [27]. For the general case the simplest method works by enumerating all possible states and has obviously an exponential time complexity. Even a system size of 4^3 is too large. Branch-and-Cut works by rewriting the problem as a linear optimization problem with an additional set of inequalities which must hold for the solution. Since not all inequalities are known *a priori* the method iteratively solves the linear problem, looks for inequalities which are violated, and adds them to the set until the solution is found. Since the number of inequalities grows exponentially with the system size the same holds for the computation time of the algorithm. Here only small systems up to 8^3 are feasible. For the spin-glass problem approximation methods like combinations of Cluster-exact approximation [28] and genetic algorithms [29,30] are more efficient: true ground states [31] up to size 14^3 can be calculated [32]. The basic idea of Cluster-exact approximation is to build sub-clusters of spins which exhibit no bond-frustration. For these subclusters the graph-theoretical methods used here can be applied, which leads to a decrease of the energy in the total system. Genetic algorithms work by minimizing many configurations of a system in parallel, keeping only those which have lower energies and creating new configurations by combining already existing configurations and flipping some spins randomly.

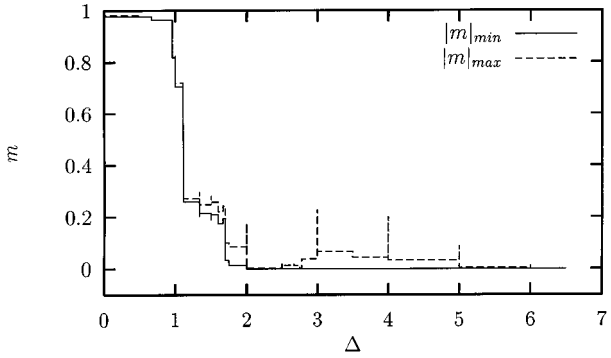

Fig. 1. Maximum and minimum of the absolute value of the staggered magnetization of a DAFF ($L = 16$, dilution 50%) *versus* field.

We now turn back to the RFIM and the DAFF. All degenerate ground states of the system are given [33] by a set of clusters and a binary relation defined on it. Each cluster is a set of antiferromagnetically (DAFF) respectively ferromagnetically (RFIM) ordered spins. These spins are not necessarily spatially connected. Two of the clusters hold the spins which have in all degenerate ground states always the same orientation. The relation describes the conditions which must hold between the orientations of the other clusters in different ground states. Using this description all degenerate ground states can be analyzed. Since all systems have a finite number of spins the ground state is a stepwise constant function of the field and, hence, this holds for the measurable quantities as well. The steps occur whenever a cluster of spins flips it orientation. In [34] it was shown that for the DAFF more than 95% of the spins do not contribute to the degeneracy. For the B-RFIM even 98% of the spins are frozen in different ground states. This is true for all fields Δ except of the finite number of fields where the ground state changes, *i.e.* a jump in a measured quantity of a single system occurs.

From the spin configurations of the ground state, we can calculate the magnetization $m = \frac{1}{L^3}\sum_i \sigma_i$ (respectively staggered magnetization for the DAFF) for a given sample. Due to the degeneracy of the ground states mentioned above the (staggered) magnetization of a certain system does not inevitably have a unique value. Instead, different degenerate ground states of a given system may have different magnetization values although the energy of the different ground states is the same, of course. Nevertheless, with our algorithm we are especially able to find exactly the maximum and the minimum value of m. In Figure 1 we show the maximum and the minimum absolute value of the staggered magnetization of one single $L = 16$ DAFF sample. The dilution of the DAFF is 50%. As discussed above, m is a stepwise constant function. It shows strong discontinuities (jumps) at integer values n of the field Δ. These jumps are due to the fact that all the single spins flip at $\Delta = n$ which are antiparallel to the field and, hence, have a local field of n generated by their n neighbors. This effect has nothing to do with the critical

[1] Implementation details: We used Tarjan's wave algorithm together with the heuristic speed-ups of Träff. In the construction of the *level graph* we allowed not only edges (v, w) with level (w) = level (v)+1, but also all edges (v, t) where t is the sink. For this measure, we observed an additional speed-up of roughly factor 2 for the systems we calculated.

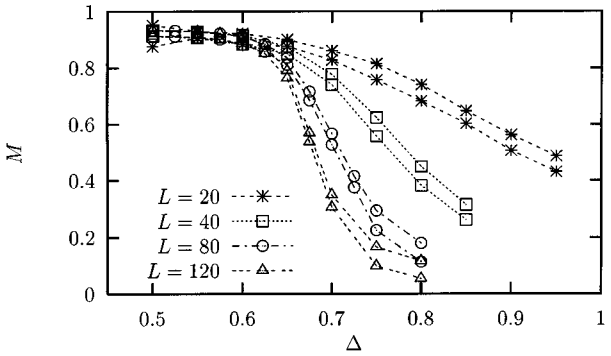

Fig. 2. Averaged maximum and minimum absolute values of the staggered magnetization *versus* field for the DAFF (dilution 55%, different system sizes).

behavior but it hinders the scaling analysis. Therefore, for the scaling analysis of the DAFF we used a higher dilution such that Δ_c is well below 1 and additionally we used larger lattice sizes such that the critical region is narrow enough so that all data we need are for values of $\Delta < 1$.

Taking the average over different disorder configurations we can calculate the order parameter $M = [|m|]$ and the disconnected susceptibility $\chi_{dis} = L^3 \left[m^2\right]$. Here, the square brackets denote an average taken over up to 180 disorder configuration for the larger system sizes and 6400 disorder configurations for the smaller systems, also depending on how close the random field strength Δ is to the critical one.

For Figure 2 we calculated the average of all maximum values as well as the average of all minimum values of m. Although these values differ significantly we checked that our results do not depend on whether we take the maximum, the minimum or an average value of the different occurring (staggered) magnetization values as far as the scaling behavior of the order parameter is concerned. Hence, we decided to neglect the effect of degeneracy and the results presented here for the order parameter and the disconnected susceptibility are taken from the maximum values of m. Note, that the considerations above do not concern the G-RFIM which exhibits a degeneracy of two only at the jumps, elsewhere it is not degenerate at all.

Apart from that Figure 2 demonstrates that for a dilution of 55% Δ_c is well below 1 so that all data we need for a finite size analysis are smooth functions without steps.

In the following analysis we use the finite size scaling relations

$$M = L^{-\beta/\nu} \tilde{M} \left((\Delta - \Delta_c) L^{1/\nu} \right) \tag{3}$$

for the order parameter and

$$\chi_{dis} = L^{\bar{\gamma}/\nu} \tilde{\chi} \left((\Delta - \Delta_c) L^{1/\nu} \right) \tag{4}$$

for the disconnected susceptibility. Figure 3 shows the corresponding scaling plots for the data of the G-RFIM.

Since both quantities, M and χ_{dis} should have the same critical field and the same correlation length exponent we adjusted Δ_c and ν for both scaling plots at the same time. From this procedure it follows $\Delta_c = 2.29 \pm 0.04$, $\nu = 1.19 \pm 0.08$, $\beta = 0.02 \pm 0.01$, and $\bar{\gamma} = 3.5 \pm 0.5$. These are values which are not surprising and in agreement with most of the previous work. The error-bars are estimated from the finite-size scaling.

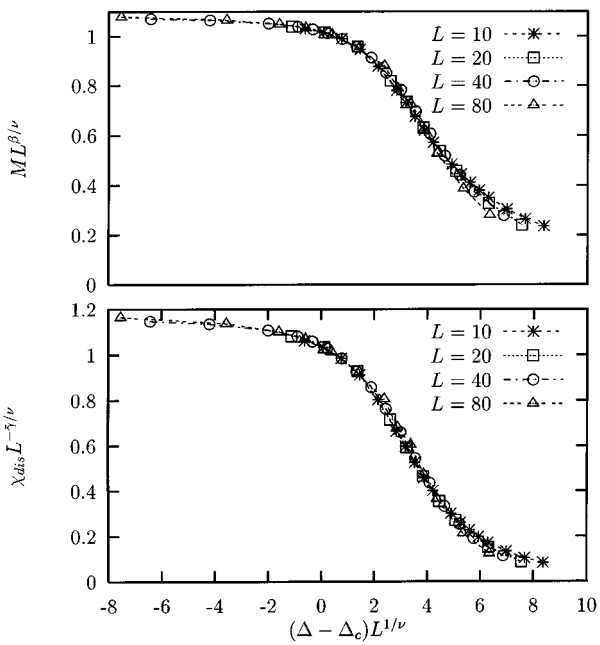

Fig. 3. Scaling plot of the magnetization and the susceptibility for the G-RFIM using $\Delta_c = 2.29$, $\nu = 1.19$, $\beta = 0.02$, and $\bar{\gamma} = 3.5$.

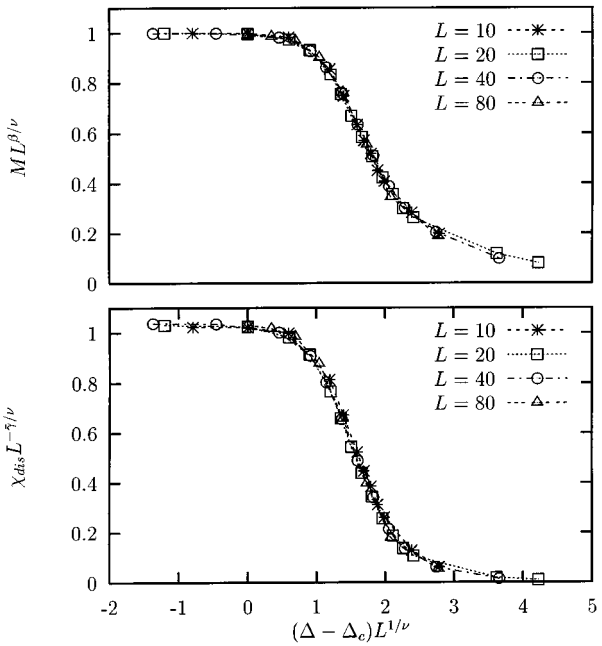

Fig. 4. Scaling plot of the magnetization and the susceptibility for the B-RFIM using $\Delta_c = 2.20$, $\nu = 1.67$, $\beta = 0.0$, and $\bar{\gamma} = 5.0$.

Figure 4 shows the same scaling plots for the data of the B-RFIM. From the scaling it follows $\Delta_c = 2.20 \pm 0.02$,

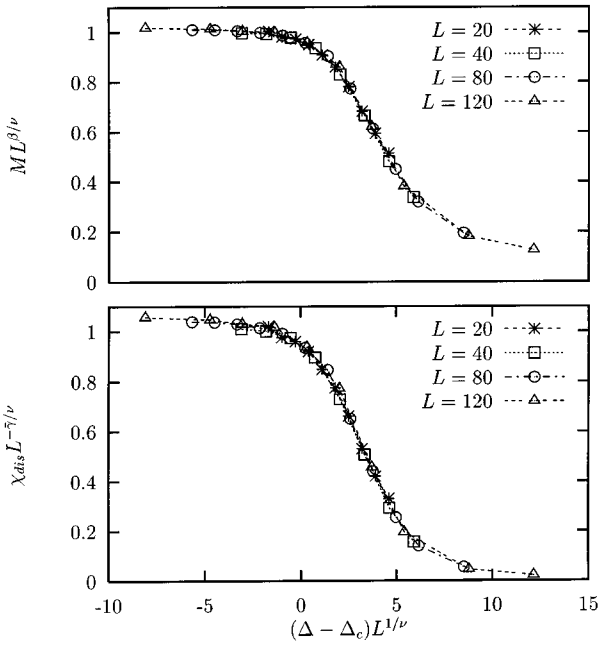

Fig. 5. Scaling plot of the staggered magnetization and the corresponding susceptibility for the DAFF using $\Delta_c = 0.62$, $\nu = 1.14$, $\beta = 0.02$, and $\bar{\gamma} = 3.4$. The unscaled data are also shown in Figure 2.

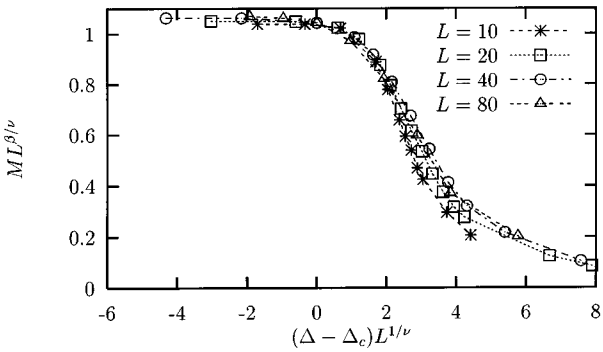

Fig. 6. Scaling plot of the magnetization with the data of the B-RFIM but with the exponents of the G-RFIM.

$\nu = 1.67 \pm 0.11$, $\beta = 0.0 \pm 0.02$, and $\bar{\gamma} = 5.0 \pm 0.4$. These values of the critical exponents differ significantly from those of the G-RFIM suggesting that the two models G-RFIM and B-RFIM are not in the same universality class. We will discuss this later in more detail. First we turn to the analysis of the data of the DAFF.

Performing the same analysis as before for the data of the DAFF results in Figure 5. Here we obtain $\Delta_c = 0.62 \pm 0.03$, $\nu = 1.14 \pm 0.10$, $\beta = 0.02 \pm 0.01$, and $\bar{\gamma} = 3.4 \pm 0.4$. These values are in good agreement with the critical exponents we found for the G-RFIM.

To prove even more clearly that the data of the B-RFIM cannot be scaled with the exponents of the DAFF or the G-RFIM we show in Figure 6 data of the B-RFIM which are scaled with the exponents of the G-RFIM and Δ_c is best-fitted. Comparing this figure with Figure 4 one can see that the data collapse is clearly worse.

The following table summarizes all results we extracted from our finite size scaling analysis.

	ν	β	$\bar{\gamma}$	Δ_c
G-RFIM	1.19±0.08	0.02±0.01	3.5±0.5	2.29±0.04
B-RFIM	1.67±0.11	0.0±0.02	5.0±0.4	2.20±0.02
DAFF	1.14±0.10	0.02±0.01	3.4±0.4	0.62±0.03

To summarize, the values we determined for the critical exponents ν, β and $\bar{\gamma}$ of the three-dimensional G-RFIM are roughly in agreement with the previous numerical works [4,35–37]. Small deviations – as far as they exist – may be due to the smaller system sizes used in earlier numerical investigations or due to the problem of equilibration of these highly disordered systems in the case of Monte-Carlo work.

The values for the critical exponents of the DAFF which we determined here for the first time within the framework of exact ground-state calculations agree within the error bars with those of the G-RFIM confirming that DAFF and G-RFIM belong to the same universality class [15,16]. Also, the value of the exponents ν and $\bar{\gamma}$ agree reasonably with experimental measurements [14].

Interestingly the values for the critical exponents of the B-RFIM deviate from those of G-RFIM and DAFF. This result as well as the values of ν are in agreement with previous numerical work [12,38]. The fact that β is zero may suggest that the phase transition is of first order as it is the case for the replica-symmetric mean-field solution [9]. It should be noted, however, that it was shown by Mezard [39] that there is replica symmetry breaking for the mean field solution of a random-field model with m-component spins in the limit of large m. In [12] it was also concluded from the exact ground-state calculations that for the three-dimensional B-RFIM the phase transition is of first order but on the other hand real space renormalization yielded deviating results concerning the order of the phase transition (see *e.g.* [40]). Also, the value of ν is even higher here. Whether the transition in the D-RFIM is of first order or not cannot be judged by our simulations.

We should mention that our results are based on a finite-size scaling analysis and in principle there is the possibility of relevant logarithmic correction to scaling which possibly could also explain the deviations of the scaling exponents of the B-RFIM from the exponents of the G-RFIM and the DAFF. However, such corrections to scaling are expected for systems at the upper or lower critical dimension of a system, a case which we do not consider here.

The modified hyperscaling-relation [41] which can be written in the form $\bar{\gamma} = D\nu - 2\beta$ where D is the spatial dimension ($D = 3$ in our case) is fulfilled by both sets of exponents.

The authors acknowledge manifold support by H. Horner, G. Reinelt, and K.D. Usadel and fruitful discussions with N. Sourlas and J.-C. Anglès d'Auriac. We are also grateful to the *Paderborn Center for Parallel Computing* for the allocation of computer time. One of the authors (AH) was supported by the Graduiertenkolleg "Modellierung und Wissenschaftliches Rechnen in Mathematik und Naturwissenschaften" at the *Interdisziplinäres Zentrum für Wissenschaftliches Rechnen* in Heidelberg and the other (UN) by the Graduiertenkolleg "Heterogene Systeme" at the *Gerhard-Mercator-Universität Duisburg*.

References

1. J.Z. Imbrie, Phys. Rev. Lett. **53**, 1747 (1984).
2. J. Bricmont, A. Kupiainen, Phys. Rev. Lett. **59**, 1829 (1987).
3. Y. Imry, S. Ma, Phys. Rev. Lett. **35**, 1399 (1975).
4. J. Esser, U. Nowak, Phys. Rev. B **55**, 5866 (1997).
5. A.J. Bray, M.A. Moore, J. Phys. C **18**, L927 (1985).
6. T. Nattermann, Phys. Stat. Sol. (b) **131**, 563 (1985).
7. J. Villain, J. Phys. France **46**, 1843 (1985).
8. U. Nowak, K.D. Usadel, J. Esser, Physica A **250**, 1 (1998).
9. A. Aharony, Phys. Rev. B **18**, 3318 (1978).
10. M.R. Swift, A. Martian, M. Cieplak, J.R. Banavar, J. Phys. A **27**, 1525 (1994).
11. M.R. Swift, A.J. Bray, A. Martian, M. Cieplak, J.R. Banavar, Europhys. Lett. **38**, 273 (1997).
12. J.-C. Anglès d'Auriac, N. Sourlas, Europhys. Lett. **39**, 473 (1997).
13. W. Kleemann, J. Mod. Phys. B **7**, 2469 (1993).
14. D.P. Belanger in *Spin Glasses and Random Fields*, edited by A.P. Young (World Scientific, 1998).
15. S. Fishman, A. Aharony, J. Phys. C **12**, L729 (1979).
16. J.L. Cardy, Phys. Rev. B **29**, 505 (1984).
17. U. Nowak, K.D. Usadel, Phys. Rev. B **44**, 7426 (1991).
18. A.N. Berker, S.R. McKay, Phys. Rev. B **33**, 4712 (1986).
19. M.N.S. Swamy, K. Thulasiraman, *Graphs, Networks and Algorithms* (Wiley, New York, 1991).
20. J.D. Claiborne, *Mathematical Preliminaries for Computer Networking* (Wiley, New York, 1990).
21. W. Knödel, *Graphentheoretische Methoden und ihre Anwendung* (Springer, Berlin, 1969).
22. J.-C. Picard, H.D. Ratliff, Networks **5**, 357 (1975).
23. J.L. Träff, Eur. J. Oper. Res. **89**, 564 (1996).
24. R.E. Tarjan, *Data Structures and Network Algorithms* (Society for industrial and applied mathematics, Philadelphia, 1983).
25. C. De Simone, M. Diehl, M. Jünger, P. Mutzel, G. Reinelt, G. Rinaldi, J. Stat. Phys. **80**, 487 (1995).
26. C. De Simone, M. Diehl, M. Jünger, P. Mutzel, G. Reinelt, G. Rinaldi, J. Stat. Phys. **84**, 1363 (1996).
27. F. Barahona, R. Maynard, R. Rammal, J.P. Uhry, J. Phys. A **15**, 673 (1982).
28. A.K. Hartmann, Physica A, **224**, 480 (1996).
29. Z. Michalewicz, *Genetic Algorithms + Data Structures = Evolution Programs* (Springer, Berlin, 1992).
30. K.F. Pál, Physica A **223**, 283 (1996).
31. A.K. Hartmann, submitted to Phys. Rev. Lett., cond-mat/9806114.
32. A.K. Hartmann, Europhys. Lett. **40**, 429 (1997).
33. J.-C. Picard, M. Queyranne, Math. Prog. Study **13**, 8 (1980).
34. A.K. Hartmann, Physica A **248**, 1 (1998).
35. A.T. Ogielski, Phys. Rev. Lett. **57**, 1251 (1986).
36. H. Rieger, Phys. Rev. B **52**, 6659 (1995).
37. M.E.J. Newman, G.T. Barkema, Phys. Rev. B **53**, 393 (1996).
38. H. Rieger, A.P. Young, J. Phys. A **26**, 5279 (1993).
39. M. Mezard, A.P. Young, Europhys. Lett. **18**, 653 (1992).
40. A. Falicov, A.N. Berker, S.R. McKay, Phys. Rev. B **51**, 8266 (1995).
41. G. Grinstein, Phys. Rev. Lett. **43**, 944 (1976).